The Direction of Tilt Aftereffects Depends on Short-term Inhibitory Facilitation

Jesus M. Cortes
DECSAI: Departamento de Ciencias de la Computacion e Inteligencia Artficial.
CITIC: Centro de Investigacion en Tecnologias de La Informacion y de las Comunicaciones
Universidad de Granada, Spain
jcortes@decsai.ugr.es

Daniele Marinazzo
Department of Data Analysis, Faculty of Psychology and Pedagogical Sciences
University of Gent, Belgium
daniele.marinazzo@ugent.be

Terrence J. Sejnowski
Howard Hughes Medical Institute
The Salk Institute, USA
Division of Biological Sciences, University of California at San Diego, USA
terry@salk.edu

Mark van Rossum
Institute for Adaptive and Neural Computation.
School of Informatics, University of Edinburgh, UK
mvanross@inf.ed.ac.uk

Abstract

Neural adaptation leads to changes in the responses of single neurons and neural populations during continued exposure to a stimulus. At the single neuron level, adaptation reduces responses to a constant stimulus. At the perceptual level, adaptation can manifest itself as aftereffects. For instance, prolonged adaptation to a grating briefly shifts the perceived orientation of a test grating, which is called the tilt aftereffect (TAE). Although phenomenological models of the perceptual effects of adaptation are common, models at the single neuron level based on physiological mechanisms resulting in TAEs at population level are rare. Here we examined a model of adaptation in populations of cortical neurons based on short-term synaptic plasticity (STP). Neurons organized in a ring model were connected by center-surround interactions. Synaptic depression, affecting both excitatory and inhibitory synapses, produced reduction in neural responses, while inhibitory facilitation increased inhibitory efficacy. For strongly facilitory synaptic inhibition the peaks of the tuning curves shifted away from the adapting stimulus (repulsive shift), but for weak inhibitory facilitation, the tuning curves shifted towards the adapting stimulus (attractive shift). Using both population vector and winner-take-all decoders, the TAE reflected in the population was attractive for high values of inhibitory facilitation and repulsive for low values. Psychophysical experiments report repulsion close to the adapting stimulus and attraction farther away, consistent with the predictions of facilitory inhibition.

1 Introduction

Adaptation is a reduction in the firing activity of neurons to prolonged stimulation that has been observed in many cortical regions of several species [1, 2, 3]. Adaptation enhances the impact of changes in sensory inputs, but in addition to reducing the responses of neurons, adaptation can also shift the tuning curves, which is thought to lead to perceptual aftereffects. Examples are the tilt aftereffect and motion aftereffects, which have been interpreted as the bias in a population decoder resulting from adaptation [4, 5, 6, 7, 8].

There are several models of adaptation that link the TAE to adaptation of the responses of single neurons and neural populations [4, 9, 8]. Here, we explore a mechanism based on short-term synaptic plasticity (STP) occurring at the same time-scale as stimulus presentation [10]. Synaptic efficacy can either increase (facilitation) or decrease (depression) in an activity-dependent manner depending on the presynaptic activity. Although the effect of synaptic depression has been studied before in the context of adaptation [11], the effect of synaptic facilitation has not been addressed before.

We study adaptation in the cortical ring model [12], in which neurons that encode different stimulus orientations are connected by lateral connections with an excitatory center-inhibitory surround profile. In presence of STP, the ring model exhibits a range of behaviors depending on the synaptic strengths. Reduction in neural responses was achieved by synaptic depression, affecting both excitatory and inhibitory connections. Synaptic facilitation affected only the inhibitory connections. Depending on the amount of facilitory inhibition, the tilt aftereffects could be either attractive or repulsive. Thus, a single parameter can change the perceptual adaptation tilts of the cortical network in either direction.

2 Modeling

2.1 Physiological data of adaptation

The adaptation parameters of the model were fitted to neural responses obtained from extracellular single unit recordings in the primary visual cortex V1 of macaque monkeys before and after adaptation to a stimulus presented for 300 ms [13]. For n = 19 different cells, 8 different orientations were tested with gratings, with both bars lighter than background and bars darker than background. The spike rate was counted in 50 ms bins. The firing rate for each orientation was calculated as the arithmetic mean across the different stimulus types. In addition, symmetric orientations (e.g. peak at +22.5 degrees and peak at -22.5 degrees) were collapsed, yielding 60 trials for the peak and the orthogonal orientation and 20 trials for all other orientations. The variability was expressed in terms of the Fano Factor (FF), which is the spike count variance across trials divided by the mean spike count. The FF did not vary with time, was independent of stimulus orientation, and did not depend on the firing rate, implying that the noise was multiplicative (see 2.2). From the data we fitted FF = 1.50 for all neurons.

2.2 Network setup and neural response

The network consisted of $N = 128$ rate-coded model neurons in a ring [12]; each neuron was labeled by its preferred orientation θ, which ranged between -90 and 90 degrees. The instantaneous firing rate $\bar{R}_\theta$ (spikes per second) was proportional to the rectified synaptic current, thus

$$\bar{R}_\theta \quad = \kappa[I]_+ + b, \tag{1}$$

where $[x]_+ = \max(x, 0)$. The constant b is the background firing rate and κ is the gain needed to produce the firing rate $\bar{R}_\theta$ for a given input I. Parameter values can be found in Table 1. The variability observed in [13] was included via multiplicative noise to each neuron's activity. This noise reflected the stochastic nature of spikes generation and was added after the input current was converted to the firing rate Eq. (1). We set

$$R_\theta = \bar{R}_\theta + \sigma(\bar{R}_\theta)\eta(t), \tag{2}$$

where η is Gaussian white noise, ($\langle\eta(t)\rangle = 0$, and $\langle\eta(t)\eta(t')\rangle = \delta_{t,t'}$), and $\bar{R}_\theta$ denotes the average over all trials. In agreement with [13], we fixed FF = 1.50 for all simulations presented here by setting the required amplitude according to $\sigma(\bar{R}_\theta) = \sqrt{1.50}\sqrt{\bar{R}_\theta}$.

Table 1: Symbols and parameters in the model

Meaning	Symbol	Value
neuron's preferred orientation	θ	$(-90, 90)$ degrees
adapting stimulus orientation	ψ	0 degrees
test orientation	ϕ	$(-90, 90)$ degrees
time decay of synaptic current	τ	10 ms
amplitude of thalamocortical input	a_{ff}	4.0
Gaussian width of thalamocortical input	σ_{ff}	45.0
gain for excitatory intracortical input	g_{exc}	3.33
interaction power for excitatory connections	A_{exc}	2.2
gain for inhibitory intracortical input	g_{inh}	125
interaction power for inhibitory connections	A_{inh}	1.4
background firing rate	b	4Hz
input current to firing rate gain	κ	4.0 Hz
Fano Factor	FF	1.5
probability of transmitter release, excitatory synapse	U_{exc}	0.02
recovery time for synaptic depression	$\tau_{\text{exc}}^{\text{dep}}$	600 ms
probability of transmitter release, inhibitory synapse	U_{inh}	0.06
recovery time for synaptic depression	$\tau_{\text{inh}}^{\text{dep}}$	100 ms
recovery time for synaptic facilitation	$\tau_{\text{inh}}^{\text{fac}}$	1 ms, 30 ms

2.3 Adaptation protocol and dynamics

For each trial, the simulation was run until the network activity reached a stationary state (~ 150ms), after which an adapting stimulus with orientation ψ was presented for 300 ms during which the network adapted, in agreement with [13], until reaching a new state in which no further adaptation was observed. The response to a stimulus with orientation ϕ was then tested, which again required the network to reach an equilibrium. The adaptation protocol is shown in Fig. 1. The activity at the end of this period corresponded to a single trial response. Decoders were applied to estimate the orientation from the population responses after 500 trials.

Thus, for each neuron the synaptic current had three angular dependencies and evolved in time according to

$$\tau \frac{\partial I(\theta, \phi, \psi, t)}{\partial t} = -I(\theta, \phi, \psi, t) + I_{\text{ff}}(\theta, \phi) + I_{\text{exc}}(\theta, \phi, \psi, t) - I_{\text{inh}}(\theta, \phi, \psi, t) \tag{3}$$

where ψ is the adapting stimulus angle, ϕ is the test stimulus angle, θ the neuron preferred orientation (the one before adaptation) and τ is the synaptic time constant [14]. The current consisted of a feedforward excitatory input I_{ff} (modeling thalamo-cortical connections) and excitatory I_{exc} and inhibitory I_{inh} inputs mediated by lateral cortical connections with a center-surround (Mexican-hat) profile subject to short-term synaptic depression and facilitation, details in 2.5.

2.4 Synaptic inputs

The input I_{ff} represented feedforward excitatory input and was assumed not to be subject to adaptation [15], and therefore to be independent on ψ. This input was modeled as a Gaussian with periodic boundary conditions:

$$I_{\text{ff}}(\theta, \phi) = a_{\text{ff}} \left[\exp\left(-\frac{(\theta - \phi)^2}{2\sigma_{\text{ff}}^2} \right) + \exp\left(-\frac{(\theta - \phi + 180)^2}{2\sigma_{\text{ff}}^2} \right) + \exp\left(-\frac{(\theta - \phi - 180)^2}{2\sigma_{\text{ff}}^2} \right) \right] \tag{4}$$

where σ_{ff} represents the Gaussian width and a_{ff} its amplitude (cf. Table 1). Lateral connections mediated the excitatory (I_{exc}) and inhibitory (I_{inh}) inputs to neuron θ according to

$$I_{\text{exc}}(\theta, \phi, \psi, t) = g_{\text{exc}} \sum_{\theta'} \mathcal{E}(\theta, \theta') u_{\text{exc}}(\theta', \phi, \psi, t) x_{\text{exc}}(\theta', \phi, \psi, t) R_{\theta'}(\phi, \psi, t)$$

$$I_{\rm inh}(\theta,\phi,\psi,t) \quad = \quad g_{\rm inh}\sum_{\theta'}\mathcal{I}(\theta,\theta')u_{\rm inh}(\theta',\phi,\psi,t)x_{\rm inh}(\theta',\phi,\psi,t)R_{\theta'}(\phi,\psi,t) \tag{5}$$

where θ' and θ represented respectively the pre- and postsynaptic neurons, the constants g were recurrent gain factors, and R_θ was a noisy realization of the firing rate.

In Eq. (5) short-term synaptic plasticity is introduced trough the dynamical variables u (facilitation) and x (depression) (see section 2.5).

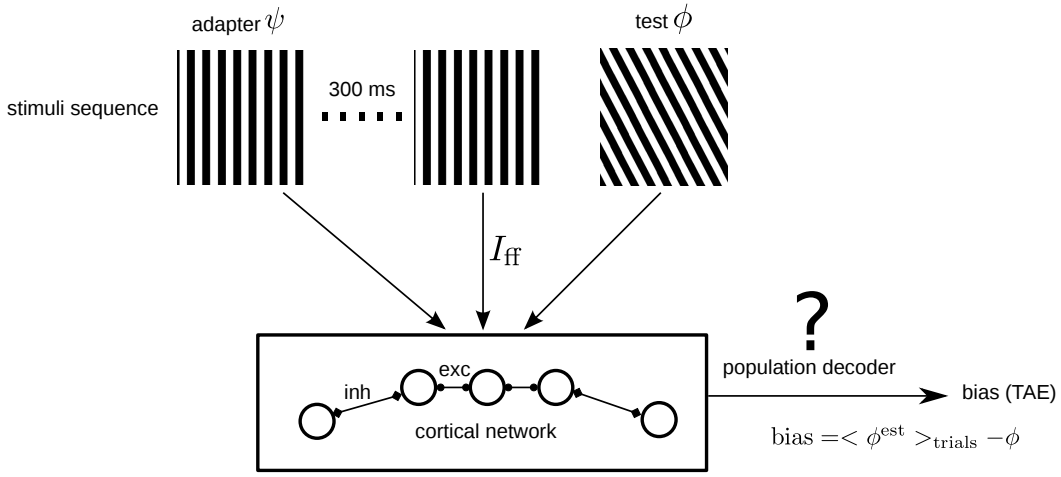

Figure 1: **Scheme for adaptation protocol and population decoder.** The network adapted to a stimulus with orientation $\psi = 0$ for 300 ms, this was followed by a test stimulus with orientation ϕ during which no further adaptation took place. The network architecture consisted of a recurrent network in which neurons received feedforward input ($I_{\rm ff}$) and lateral input with short range excitation (exc, connection with circles) and long range inhibition (inh, diamonds). Periodic boundary conditions (not shown) ensured a ring topology for the network. Reading out the population response by a decoder, we computed the bias (a proxy for the TAE) for both nonfacilitory inhibition and facilitory inhibition.

The functions $\mathcal{E}$ and $\mathcal{I}$ in Eq. (5) define the connection strength between cells θ and θ'. Similar to [9], we use $\mathcal{E}(\theta,\theta') = [CK(|\theta-\theta'|)]_+$ and $\mathcal{I}(\theta,\theta') = [-CK(|\theta-\theta'|)]_+$ where $K(\theta) = [\cos(2\theta)+1]^{A_{\rm exc}} - [\cos(2\theta)+1]^{A_{\rm inh}}$. The functions $\mathcal{E}$ and $\mathcal{I}$ were normalized with the constant C so that the sum of connections from any cell to the rest equals 1, that is $1/C = \sum_i |K(\theta_i)|$. The exponents $A_{\rm exc}$ and $A_{\rm inh}$ control the range of interaction; the smaller they are, the flatter and wider the connection profile. We used a center-surround or Mexican-hat profile for the connection, satisfying $A_{\rm exc} > A_{\rm inh}$, as in previous studies [12, 9, 16].

2.5 Synaptic short-term plasticity as a potential mechanism for cortical adaptation

According to the phenomenological model in [10], synaptic efficacy is modulated by synaptic depression (x) and synaptic facilitation (u). Physiologically, the dynamics of x accounts for neurotransmitters depletion and u for the calcium influx into the presynaptic terminal and its effects on release probability (U). The amount of available resources is given by x and the utilization parameter by u. First-order differential equations for the depression dynamics gives

$$\frac{\partial x(\theta,\phi,\psi,t)}{\partial t} = \frac{1-x(\theta,\phi,\psi,t)}{\tau^{\rm dep}} - u(\theta,\phi,\psi,t)x(\theta,\phi,\psi,t)R_\theta(\phi,\psi,t) \tag{6}$$

According to Eq. (5), for a given neuron response R_θ, an amount ux of neurotransmitters is integrated into the postsynaptic current, thus reducing x. At the same time, the response R_θ increases u according to

$$\frac{\partial u(\theta,\phi,\psi,t)}{\partial t} = \frac{U-u(\theta,\phi,\psi,t)}{\tau^{\rm fac}} + U\left(1-u(\theta,\phi,\psi,t)\right)R_\theta(\phi,\psi,t). \tag{7}$$

Both parameters τ^{fac} and τ^{dep} are recovery time constants, that is, the variables u and x recover respectively to baselines given by $u = U$ and $x = 1$. Thus, for each synapse the limits for x are 0 for maximum depression and 1 for zero-depression. The limits for u are U for zero-facilitation and 1 for maximum facilitation. Between those limits, both dynamical variables x and u evolves in time in an activity-dependent manner according to Eqs. (6) and (7).

Although in principle both excitatory and inhibitory synapses may exhibit synaptic depression combined with synaptic facilitation [17], we will consider assume that excitatory synapses are depressing, while inhibitory synapses display both depression and facilitation. To tune the strength of facilitation we set $\tau^{\text{fac}}_{\text{inh}} = 30$ ms to obtain strong facilitation. We used $\tau^{\text{fac}}_{\text{inh}} = 1$ ms for very weak facilitation; the recovery is then so fast that facilitation is virtually absent.

3 Results

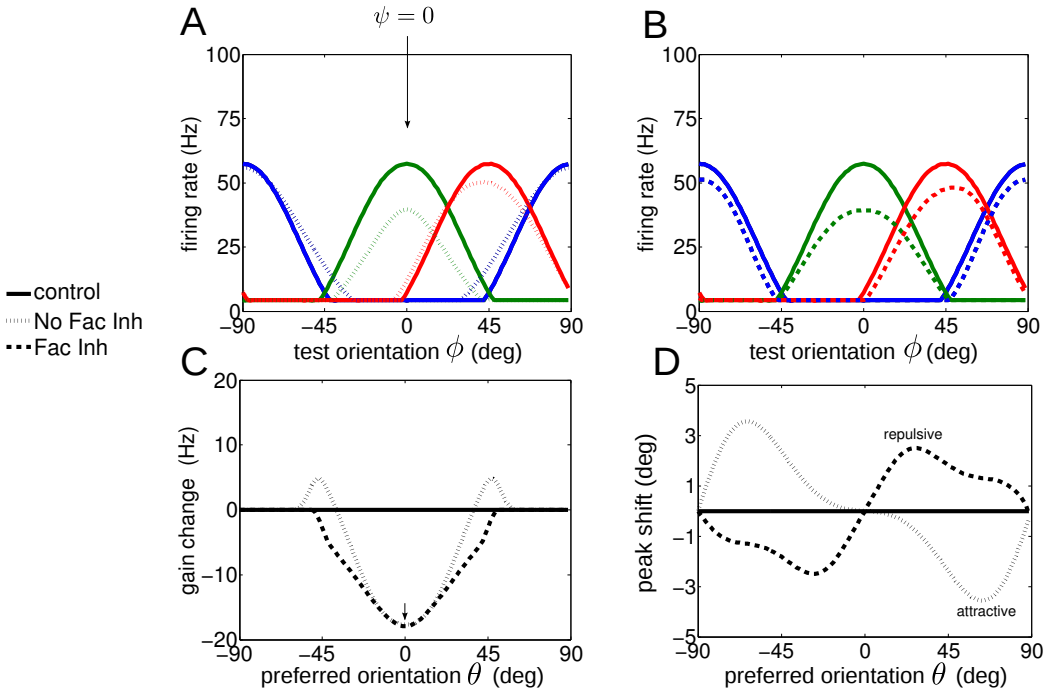

Figure 2: **Effect of adaptation on population response.** A,B: Tuning curve properties at the non-facilitory inhibition (A) and facilitory inhibition (B). Individual neuron tuning curves before and after adaptation for neurons with a preferred orientation of 0 (green), 45 (red) and 90 (blue) degrees, before (solid lines) and after adaptation (dashed lines). The adapting stimulus orientation ψ was at zero degrees (marked with an arrow in panel A). C,D: Changes in tuning curve properties after adaptation. C: Gain change for all neurons, defined as the difference between the maximal response per neuron after adaptation and the response before adaptation. The model parameters in the two conditions A and B were chosen in order to produce the same gain change for the neuron with $\theta = 0$ (marked with a small arrow). D: Peak position shift for all the neurons, defined as the difference between the location of the center of mass of each neuron's tuning curve after and before adaptation. For neurons with positive preferred orientations, positive values for the peak shift correspond to repulsive shifts (away from the adapting stimulus) and negative values to attractive shifts (towards the adapting stimulus). The two conditions A and B, only differing by the amount of short-term synaptic inhibitory facilitation, yielded different shift directions after adaptation.

We first examined the effects of the STP on the tuning curves Fig.2. In both STP scenarios the peak firing rates were reduced after adaptation. However, the feet of the tuning curves were differently modified, Fig.2C. The peak shift of the tuning curves was also strongly dependent on the facilitation strength, Fig.2D.

Next, we analyzed how adaptation modified the output of the network. Fig. 3. We estimated the decoding performance with two well-known population decoders, the Population Vector (PV) and Winner-Take-All (WTA) [4]. Since these decoders do not have access to the state of adaptation, their estimates will typically be biased [7]. For winner-take-all decoding the estimate was simply the (non-adapted) preferred orientation of the neuron with highest firing rate. For the population vector decoder the responses of all neurons were vectorially summed with an orientation equal to the neuron's preferred orientation before adaptation.

For each decoder, we computed both the bias and the variance. The bias is the difference between the mean perceived orientation and the actual presented stimulus orientation. Similar to previous works [4, 5, 8], the bias of the decoder can be interpreted as the tilt aftereffect (TAE). For estimations of positive test orientations ($\phi > 0$), positive values of the bias give a repulsive TAE and negative values an attractive TAE. The decoder variance is a measure of its efficiency, the smaller it is the more efficient is the decoder [7].

For the two decoders, the bias had a similar profile, Fig. 3A-B top row. The case of nonfacilitory inhibition always gave a repulsive TAE from the adapting stimulus, independently on the orientation of test stimuli. For the case of facilitory inhibition, however, both repulsive and attractive TAEs occurred. Nearby to the adapting stimulus ψ, a small repulsive TAE coexisted with an attractive TAE further from the adapting stimulus. As previously reported, the tuning of individual neurons can behave differently from the population tuning [9]. The population bias can be opposite from the individual tuning curve shift, cf. Fig. 3A-B to Fig. 2D. The reason is that the population vector weights individual responses according to their firing rate. Therefore, although a neural tuning curve could shift towards the adapting stimulus orientation, if the rate were sufficiently reduced, the population vector can instead shift away from the orientation of the adapting stimulus.

The variance of the two decoders as a measure of their efficiency is plotted in Fig. 3 (bottom row). The variance of both decoders was greatest at orientations close to the adapting stimulus compared to orthogonal test orientations, where the response reduction is largest, Fig. 2C.

4 Discussion

The ring model with STP replicated perceptual tilt aftereffects and links them to changes in the orientation tuning curves of neurons. Adaptation of firing rates was driven by synaptic depression at both the excitatory and inhibitory synapses. Synaptic facilitation of inhibitory connections affected the tilt direction of the aftereffects. The bias and variance of two population decoders were computed with and without facilitory inhibition. These two conditions yielded different TAEs. Without inhibitory facilitation, the two decoders predicted a strong repulsive TAE. However, repulsive and attractive shifts were predicted with inhibitory facilitation by both decoders. Psychophysical experiments report repulsion close to the adapting stimulus and attraction far away from it [18, 5, 8], consistent with the predictions of facilitory inhibition. The variance of both decoders was highest for orientations close to the adapting stimulus, independently of the facilitation. This prediction is consistent with better performance at test angles orthogonal to the adapting stimulus compared to the performance for test orientations close to the adapter [19, 7].

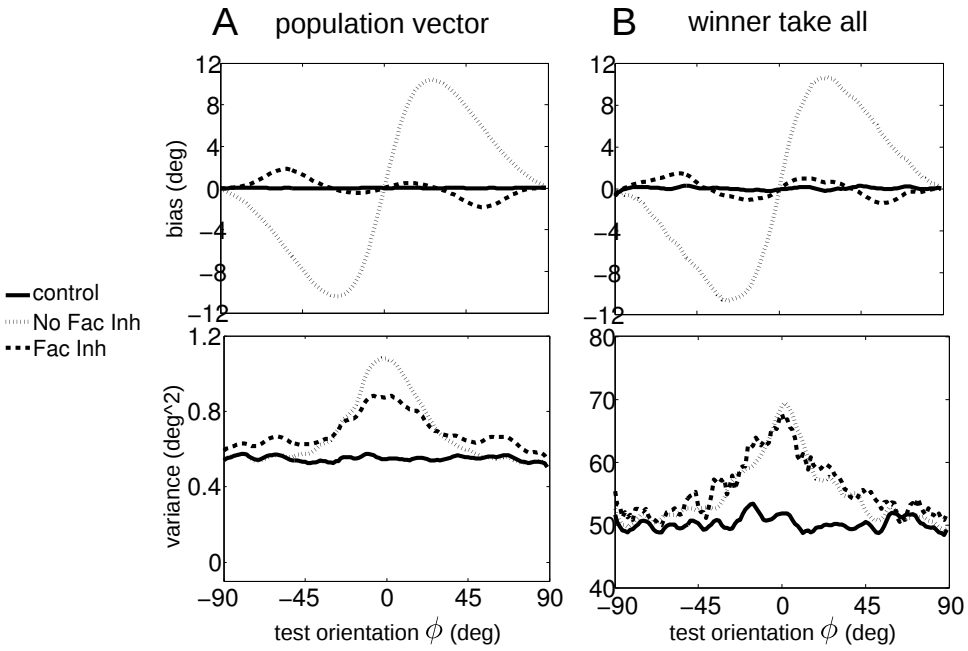

Figure 3: **Effect of adaptation on decoders and the tilt aftereffect.** For the A, population vector (PV) and B, winner-take-all (WTA) decoders we computed the bias due to the adaption, which is a measure of the tilt aftereffect (TAE). The bias (top row) is similar for the two decoders: after adaptation there was a strong repulsive TAE for the case of nonfacilitory inhibition. For facilitory inhibition it is possible to have both a small repulsive TAE for test orientations close to the adapting stimulus and an attractive shift for orientations farther from the adapting stimulus. The variance (bottom row) gives an idea of the efficiency of the decoder. If after many trials with the same conditions the estimation does not differ among all repetitions, the decoder is efficient. Both decoders were qualitatively similar. For orientations close to the adapting stimulus, the two decoders performed less efficiently compared to the testing of orthogonal orientations to the adapting stimulus. Although the average bias was comparable for the two decoders, the WTA variance was much higher, which means it was much less efficient than the PV.

References

[1] I. Ohzawa, G. Sclar, and R.D. Freeman. Contrast gain control in the cat visual cortex. *Nature*, 298:266268, 1982.

[2] Z.S. Shu, N.V. Swindale, and M.S. Cynader. Spectral motion produces an auditory after-effect. *Nature*, 364:721723, 1993.

[3] M. Carandini and D. Ferster. A tonic hyperpolarization underlying contrast adaptation in cat visual cortex. *Science*, 276:949952, 1997.

[4] Dezhe Z Jin, Valentin Dragoi, Mriganka Sur, and H. Sebastian Seung. Tilt aftereffect and adaptation-induced changes in orientation tuning in visual cortex. *J Neurophysiol*, 94(6):4038–4050, Dec 2005.

[5] Odelia Schwartz, Anne Hsu, and Peter Dayan. Space and time in visual context. *Nat Rev Neurosci*, 8(7):522–535, Jul 2007.

[6] A. Kohn. Visual adaptation: physiology, mechanisms, and functional benefits. *J Neurophysiol*, 97:3155–3164, 2007.

[7] Peggy Seriès, Alan A Stocker, and Eero P Simoncelli. Is the homunculus "aware" of sensory adaptation? *Neural Comput*, 21(12):3271–3304, Dec 2009.

[8] Odelia Schwartz, Terrence J Sejnowski, and Peter Dayan. Perceptual organization in the tilt illusion. *J Vis*, 9(4):19.1–1920, 2009.

[9] A.F. Teich and N. Qian. Learning and adaptation in a recurrent model of v1 orientation selectivity. *J Neurophysiol*, 89:2086–2100, 2003.

[10] Gianluigi Mongillo, Omri Barak, and Misha Tsodyks. Synaptic theory of working memory. *Science*, 319(5869):1543–1546, Mar 2008.

[11] J.M. Cortes, D. Marinazzo, P. Series, M.W. Oram, T.J. Sejnowski, and M.C.W. van Rossum. Neural adaptation reduces energy cost while preserving coding accuracy. Society for Neuroscience Annual Meeting, 2010.

[12] R. Ben-Yishai, R. Lev Bar-Or, and H. Sompolinksy. Theory of orientation tuning in visual cortex. *Proc Natl Acad Sci USA*, 92:3844–3848, 1995.

[13] M. W. Oram, M. C. Wiener, R. Lestienne, and B. J. Richmond. Stochastic nature of precisely timed spike patterns in visual system neuronal responses. *J. Neurophysiol.*, 81:3021–3033, 1999.

[14] P. Dayan and L.F. Abbott. *Theoretical Neuroscience*. The MIT Press, 2001.

[15] C.E. Boudreau and D. Ferster. Short-Term Depression in Thalamocortical Synapses of Cat Primary Visual Cortex. *J Neurosci*, 25:7179 7190, 2005.

[16] P. Seriès, P. E Latham, and A. Pouget. Tuning curve sharpening for orientation selectivity: coding efficiency and the impact of correlations. *Nat Neurosci*, 7(10):1129–1135, Oct 2004.

[17] A.M. Thomson and C. Lamy. Functional maps of neocortical local circuitry. *Front Neurosci*, 1:19–42, 2007.

[18] C.W.G. Clifford, P. Wenderoth, and B. Spehar. A functional angle on some after-effects in cortical vision. *Proc R Soc Lond B*, 267(1454):1705–1710, 2000.

[19] C. W. Clifford, A. M. Wyatt, D. H. Arnold, S. T. Smith, and P. Wenderoth. Orthogonal adaptation improves orientation discrimination. *Vision Res*, 41(2):151–159, Jan 2001.